

# Highly Efficient Electrophosphorescent Devices with Saturated Red Emission from a Neutral Osmium Complex

Yu-Hua Niu,<sup>†</sup> Yung-Liang Tung,<sup>‡</sup> Yun Chi,<sup>‡</sup> Ching-Fong Shu,<sup>§</sup> Joo Hyun Kim,<sup>†</sup>  
Baoquan Chen,<sup>†</sup> Jingdong Luo,<sup>†</sup> Arthur J. Carty,<sup>||</sup> and Alex K.-Y. Jen<sup>\*,†</sup>

Department of Materials Science and Engineering, Box 352120, University of Washington, Seattle, Washington 98195, Department of Chemistry, National Tsing Hua University, Hsinchu 300, Taiwan, Department of Applied Chemistry, National Chiao Tung University, Hsinchu 30035, Taiwan, and Steacie Institute for Molecular Sciences, National Research Council Canada, Ontario K1A 0R6, Canada

Received December 30, 2004. Revised Manuscript Received April 19, 2005

Highly efficient electrophosphorescent polymer light-emitting diodes (LEDs) with saturated red emission (Commission Internationale de L'Eclairage chromaticity coordinates exactly at  $x = 0.67$ ,  $y = 0.33$ ) are achieved by blending a novel neutral Osmium complex into a single-component bipolar polymer host that possesses balanced hole- and electron-transporting ability. By using a tetraphenylenebiphenyldiamine (TPD)-based cross-linkable hole-transport layer as well as a layer of 1,3,5-tris(*N*-phenylbenzimidazol-2-yl)benzene (TPBI) as an electron-transport layer, a device structure with both effective hole/electron injection and efficient carriers/excitons blocking or confinement at both electrode sides is constituted. In this way, external quantum efficiency 12.8% is reached the first time with an organometallic complex with heavy metal core other than iridium.

## Introduction

Organic and polymer light-emitting diodes (LEDs) have recently made very significant progress toward applications in full-color flat-panel displays.<sup>1</sup> One of the challenging tasks in achieving high-quality displays is to obtain very efficient LEDs with saturated red emission with Commission Internationale de L'Eclairage (CIE) chromaticity coordinates at  $x = 0.67$ ,  $y = 0.33$ . Previously, saturated red emission with external quantum efficiency ( $\eta_{\text{ext}}$ ) of more than 3.8 photon/electron (ph/el) % was reported for a fluorescent polymer.<sup>2</sup> However, according to simple spin-pairing statistics, the singlet formation probability in the charge recombination process of fluorescent LEDs is only 25%, although this ratio might be higher in conjugated polymers.<sup>3</sup> This limits further performance enhancement of fluorescent emitters-based LEDs.

To overcome the upper limit of singlet-exciton formation, phosphorescent dopants have been successfully used in organic LEDs to facilitate the harvest of both the singlet and the triplet excitons, thus providing the opportunity to realize an internal quantum efficiency of close to 100% ( $\eta_{\text{ext}} = 19\text{--}20$  ph/el %) for the iridium complex based green emitter.<sup>4</sup>

Very efficient red-emitting electrophosphorescent LEDs employing iridium complexes doped in a host of small molecules have also been reported by Adachi, Su, and Tsuboyama, showing near saturated red ( $x = 0.68$ ,  $y = 0.32$ ) emission with very high  $\eta_{\text{ext}}$  (7–10.3 ph/el %).<sup>5</sup> Recently, Jiang et al. demonstrated saturated red ( $x = 0.67$ ,  $y = 0.33$ ) LEDs with  $\eta_{\text{ext}} = 12$  ph/el % by doping bis(2-phenylquinolyl)-*N,C*(<sup>2'</sup>) iridium (acetylacetonate) into hosts composed of blends of polymer and electron-transporting small organic molecules.<sup>6</sup>

However, for most of these LEDs, the device quantum efficiency drops rapidly with increasing current density and consequently with increasing brightness. Due to the long phosphorescent lifetime, triplet excitons relax more slowly and can potentially cause saturation of the emission sites. Baldo et al. proved that the major quenching mechanism in phosphorescent LEDs is triplet–triplet (T–T) annihilation.<sup>7</sup> One way to alleviate the problem is to use phosphorescent dopants with shorter triplet exciton lifetime. The widely used Ir complexes often have phosphorescence lifetime ranging from 1 to 11  $\mu\text{s}$ .<sup>8</sup> However, since Os complexes have shorter

\* To whom correspondence should be addressed. E-mail: ajen@u.washington.edu.

<sup>†</sup> University of Washington.

<sup>‡</sup> National Tsing Hua University.

<sup>§</sup> National Chiao Tung University.

<sup>||</sup> National Research Council Canada.

- (1) (a) Burroughes, J. H.; Bradley, D. D. C.; Brown, A. R.; Marks, R. N.; MacKay, K.; Friend, R. H.; Burn, P. L.; Holmes, A. B. *Nature* **1990**, *347*, 539. (b) Gustafsson, G.; Cao, Y.; Treacy, G. M.; Klavetter, F.; Colaneri, N.; Heeger, A. J. *Nature* **1992**, *357*, 477.
- (2) Niu, Y.-H.; Huang, J.; Cao, Y. *Adv. Mater.* **2003**, *15*, 807.
- (3) (a) Cao, Y.; Parker, I. D.; Yu, G.; Zhang, C.; Heeger, A. J. *Nature* **1999**, *397*, 414. (b) Wohlgenannt, M.; Tandon, K.; Mazumdar, S.; Ramasesha, S.; Vardeny, Z. V. *Nature* **2001**, *409*, 494.

- (4) (a) Adachi, C.; Baldo, M. A.; Thompson, M. E.; Forrest, S. R.; *J. Appl. Phys.* **2001**, *90*, 5048. (b) Ikai, M.; Tokito, S.; Sakamoto, Y.; Suzuki, T.; Taga, Y. *Appl. Phys. Lett.* **2001**, *79*, 156.

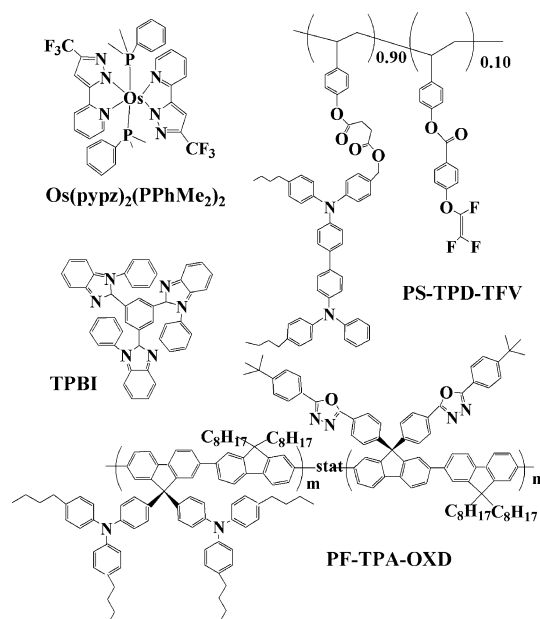
- (5) (a) Adachi, C.; Baldo, M. A.; Forrest, S. R.; Lamansky, S.; Thompson, M. E.; Kwong, R. C. *Appl. Phys. Lett.* **2001**, *78*, 1622. (b) Su, Y.-J.; Huang, H.-L.; Li, C.-L.; Chien, C.-H.; Tao, Y.-T.; Chou, P.-T.; Satta, S.; Liu, R.-S. *Adv. Mater.* **2003**, *15*, 884. (c) Tsuboyama, A.; Iwawaki, H.; Furugori, M.; Mukaide, T.; Kamatani, J.; Igawa, S.; Moriyama, T.; Miura, S.; Takiguchi, T.; Okada, S.; Hoshino, M.; Ueno, K. *J. Am. Chem. Soc.* **2003**, *125*, 12971.

- (6) Jiang, C.; Yang, W.; Peng, J.; Xiao, S.; Cao, Y. *Adv. Mater.* **2004**, *16*, 537.

- (7) Baldo, M. A.; Adachi, C.; Forrest, S. R. *Phys. Rev. B* **2000**, *62*, 10967.

- (8) Lamansky, S.; Djurovich, P.; Murphy, D.; Abdel-Razzaq, F.; Lee, H.-E.; Adachi, C.; Burrows, P. E.; Forrest, S. R.; Thompson, M. E. *J. Am. Chem. Soc.* **2001**, *123*, 4304.

**Scheme 1. Chemical Structures of the Os Complex, Os(pypz)<sub>2</sub>(PPhMe<sub>2</sub>)<sub>2</sub> (Os–R), the Cross-linkable Precursor of the Hole-Transport Material, PS–TPD–TFV, the Electron-Transport Material, TPBI, and the Host Polymer, PF–TPA–OXD**



exciton lifetime, usually less than 1  $\mu\text{s}$ ,<sup>9</sup> it is possible to use them for highly efficient red LEDs.

In this work highly efficient red LEDs were fabricated by doping a neutral Os complex, Os(pypz)<sub>2</sub>(PPhMe<sub>2</sub>)<sub>2</sub> (Os–R, Scheme 1), into a bipolar conjugated polymer without adding any additional charge-transporting small molecules to balance carrier transport. A very high external quantum efficiency (12.8 ph/el %) and high brightness (>19000 cd/m<sup>2</sup>) were realized with CIE coordinates at  $x = 0.67$  and  $y = 0.33$ . To our knowledge, these results represent one of the best values reported for red LEDs with a phosphorescent emitter hosted in a single-component conjugated polymer.

## Experimental Section

**General Details on Synthesis of the Os Complex.** Blue-emitting Os complex, [Os(pypz)<sub>2</sub>(CO)<sub>2</sub>] (200 mg, 0.25 mmol),<sup>10</sup> freshly sublimed Me<sub>3</sub>NO (90 mg, 1.19 mmol) to eliminate the coordinated CO ligands, and phosphine ligand PPhMe<sub>2</sub> (0.43 mL, 2.98 mmol) were used as starting materials to synthesize Os–R. All reactions were performed under nitrogen. After the reaction was finished, the content was washed with water, followed by silica gel column chromatography, and re-crystallized from hexane solution to afford the dark red crystalline solid with 55% yield.

**Optical Properties Test.** Ultraviolet–visible (UV–Vis) spectra of the spin-coated solid-state films were recorded on a Perkin-Elmer spectrophotometer (Lambda 9 UV/vis/NIR). Photoluminescence (PL) spectra were obtained by exciting the films at wavelength of 336 nm and the emission was collected with an Oriel Instaspec IV charge-coupled device (CCD) detector.

**Device Fabrication and Test.** The devices were fabricated on indium tin oxide (ITO)-coated glass substrates with sheet resistance  $\sim 20 \Omega/\square$ . The substrates are ultrasonicated sequentially in detergent, deionized water, 2-propanol, and acetone and are treated with O<sub>2</sub> plasma for 10 min before use. A layer of the thermally cross-linkable precursor, PS–TPD–TFV with both thermally curable trifluorovinyl ether (TFV) group and hole-transporting TPD group as side branches attached on the polystyrene main chain (Scheme 1), in 1,2-dichloroethane with the concentration of 5 mg/mL was spin-coated onto ITO and was thermally cross-linked at 235 °C for 40 min under argon to form a solvent-resistant layer.<sup>11</sup> For the control devices, a layer of commercial available polyethylene dioxythiophene polystyrene sulfonate (PEDOT:PSS, Bayer AG) film was spin-coated on ITO. The electroluminescent (EL) layer was then spin-coated on top of the cross-linked PS–TPD–TFV layer or PEDOT:PSS layer. Measured by a Sloan Dektak 3030 surface profiler, the thickness of the PS–TPD–TFV or PEDOT:PSS film was  $\sim 30$  nm, and the thickness of the EM layer was  $\sim 40$  nm. In a vacuum below  $1 \times 10^{-6}$  Torr, 1,3,5-tris(*N*-phenylbenzimidazol-2-yl)benzene (TPBI, Scheme 1,  $\sim 25$  nm) was sublimed. Cesium fluoride with thickness of 1 nm and aluminum of 20 nm were evaporated subsequently as cathode.<sup>12</sup>

The device testing was carried out in air at room temperature. EL spectra were recorded by the Oriel Instaspec IV spectrometer with a CCD detector. Current–voltage ( $I$ – $V$ ) characteristics were measured on a Hewlett-Packard 4155B semiconductor parameter analyzer. The power of EL emission was measured using a calibrated Si photodiode and a Newport 2835-C multifunctional optical meter. Photometric units (cd/m<sup>2</sup>) were calculated using the forward output power together with the EL spectra of the devices under assumption of the emission's Lambertian space distribution.<sup>13</sup> One data point recalibration was made with the brightness tested from a PR-650 SpectraColorimeter (Photo Research Co.) with LEDs operating at current density of 10 mA/cm<sup>2</sup>. The CIE coordinates were measured with the PR-650 at the same time.

## Results and Discussion

**Structural Characteristics of the Os Complex.** The Os complex consists of two chelating anions of 3-trifluoromethyl-5-(2-pyridyl) pyrazole (pypz) to balance the +2 charge on the metal cation, and two phosphine donors located at the trans positions to complete the coordination requirement.<sup>14</sup> In contrast to ionic Os(II) emitters in which the injected holes and electrons may be strongly coupled to the counterions,<sup>9b</sup> this Os complex is a discretely neutral molecule, which can lead to more efficient carrier direct-trapping and recombination.<sup>9d</sup> Detailed structural characterization data can be found from ref 14.

**Blends Preparation.** As EL layer in LEDs, it is crucial to blend the triplet emitter into a suitable host that transports both the positive and negative carriers into the EL layer. Excitons that are formed in the host can also migrate to the

- (9) (a) Carlson, B.; Phelan, G. D.; Kaminsky, W.; Dalton, L.; Jiang, X.; Liu, S.; Jen, A. K.-Y., *J. Am. Chem. Soc.* **2002**, *124*, 14162. (b) Ma, Y. G.; Zhang, H. Y.; Shen, J. C.; Che, C. M. *Synth. Met.* **1998**, *94*, 245. (c) Jiang, X.; Jen, A. K.-Y.; Carlson, B.; Dalton, L. *Appl. Phys. Lett.* **2002**, *81*, 3125. (d) Jiang, X.; Jen, A. K.-Y.; Carlson, B.; Dalton, L. *Appl. Phys. Lett.* **2002**, *80*, 713.
- (10) Wu, P.-C.; Yu, J.-K.; Song, Y.-H.; Chi, Y.; Chou, P.-T.; Peng, S.-M.; Lee, G.-H. *Organometallics* **2003**, *22*, 4938.

- (11) (a) Jiang, X.; Liu, S.; Liu, M. S.; Hergurth, P.; Jen, A. K.-Y.; Fong, H.; Sarikaya, M. *Adv. Funct. Mater.* **2002**, *12*, 745. (b) Liu, S.; Kim, J. H.; Niu, Y.-H.; Luo, J. D.; Jen, A. K.-Y. Submitted to *Macromolecules*.
- (12) Brown, T. M.; Friend, R. H.; Millard, I. S.; Lacey, D. J.; Burroughes, J. H.; Cacialli, F. *Appl. Phys. Lett.* **2001**, *79*, 174.
- (13) Greenham, N. C.; Friend, R. H.; Bradley, D. D. C. *Adv. Mater.* **1994**, *6*, 491.
- (14) Tung, Y.-L.; Wu, P.-C.; Liu, C.-S.; Chi, Y.; Yu, J.-K.; Hu, Y.-H.; Chou, P.-T.; Peng, S.-M.; Lee, G.-H.; Tao, Y.; Carty, A. J.; Shu, C.-F.; Wu, F.-I. *Organometallics* **2004**, *23*, 3745.

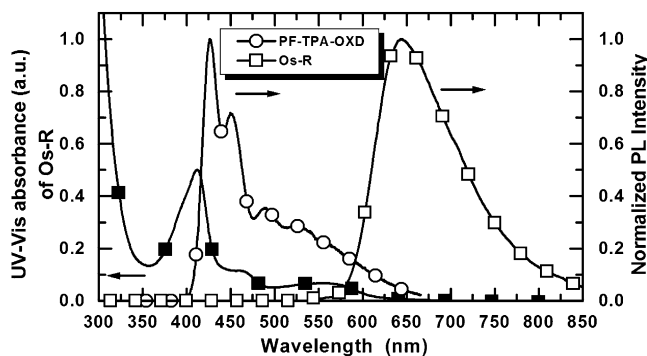


**Figure 1.** UV-Vis absorbance (■) and PL spectra (□) of the Os complex, Os-R, overlapped with the PL spectrum of the host, PF-TPA-OXD (○).

triplet dopant via the Förster or the Dexter energy transfer processes.<sup>15</sup> Alternatively, charge carrier can be directly trapped by the guest and wait for the opposite carrier to recombine.<sup>16</sup> A host with balanced electron and hole transport abilities will be beneficial for both mechanisms. The highly efficient blue-emitting conjugated polymer with fluorene backbone and triphenylamine (TPA) and oxadiazole (OXD) as side chains (PF-TPA-OXD, Scheme 1) is chosen as the host because of its TPA-based hole transport ability and OXD-based electron transport ability.<sup>17</sup> Solution blending of Os-R in PF-TPA-OXD was carried out at specific volume ratios using separate solution matrixes with a concentration of 10 mg/mL in tetrahydrofuran and chlorobenzene, respectively. Compared with the multisources co-sublimation for small molecules, the solution blending method can have the ratio controlled precisely. Meanwhile, the high glass transition temperature of PF-TPA-OXD, 155 °C,<sup>17</sup> can potentially provide the blends with good thermal stability.

**Optical Properties.** UV-Vis and PL spectra of Os-R in solid films are shown in Figure 1. The absorption peaks around 410, 465, and 550 nm correspond to the typical spin-allowed metal to ligand charge transfer (<sup>1</sup>MLCT) transition and the spin-orbit coupling enhanced <sup>3</sup> $\pi\pi^*$  and <sup>3</sup>MLCT transitions, respectively. The PL spectrum peaks at 648 nm render the saturated red emission. The phosphorescent lifetime measured in solid film state at room temperature is 0.61  $\mu$ s, which is considerably shorter than that of the commonly reported red-emitting Ir(III) complexes.<sup>18</sup>

The partial overlap between the PL spectrum of PF-TPA-OXD and the <sup>1</sup>MLCT absorption spectrum of Os-R (Figure 1) implies that the energy transfer from the host to the guest might happen only at a moderate level. Consistent with this, as shown by the PL spectra of the spin-coated films of the Os-R:PF-TPA-OXD blends in different ratios (Figure 2a), the emission from the host cannot be completely quenched even with more than 8 wt % of Os-R.

**Device Properties.** To realize high efficiency, it is important to have effective mechanisms for both hole- and

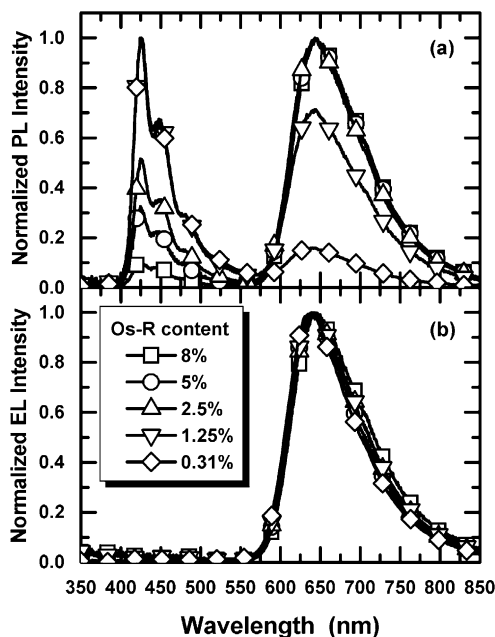
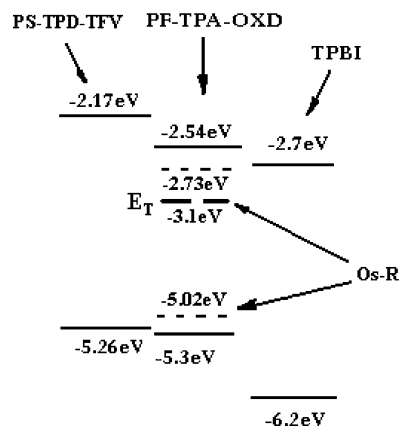


**Figure 2.** (a) PL spectra of the spin-coated films of the Os-R:PF-TPA-OXD blends in different ratios and (b) EL spectra from LEDs with those blends as EL layer.

**Scheme 2. Demonstration of Energy Levels of the Materials in Concern<sup>11,17,20</sup> ( $E_T$  Means the Triplet Energy Level Position of Os-R)**



electron-blocking as well as exciton confinement at both electrodes. Although it was suggested by Kan et al. that the triplet exciton-blocking layer (EBL) might not be required for the polymer-hosted system because the polymer host can limit the diffusion and annihilation of triplet excitons,<sup>19</sup> the negation of the EBL necessitates a thick EL layer, leading to higher turn-on and driving voltages.<sup>6,20</sup> With utilization of a hole-transporting layer (HTL) and an electron-transporting layer (ETL) at both electrode sides, very high efficiency and brightness can be realized at low driving voltage. Therefore, we employed the cross-linkable hole-transporting polymer (PS-TPD-TFV) as HTL.<sup>11</sup> As perceived in Scheme 2, this layer also functions as an electron-blocking and exciton-confining layer at the anode side. Meanwhile, at the cathode side, a layer of TPBI was used as ETL (Scheme 1).<sup>21</sup> As shown in Scheme 2, this layer can also

(15) (a) Förster, T. *Discuss. Faraday Soc.* **1959**, 27, 7. (b) Dexter, D. L. *J. Chem. Phys.* **1953**, 21, 836.

(16) Gong, X.; Ostrowski, J. C.; Moses, D.; Bazan, G. C.; Heeger, A. J. *Adv. Funct. Mater.* **2003**, 13, 439.

(17) Shu, C.-F.; Dodda, R.; Wu, F.-I.; Liu, M. S.; Jen, A. K.-Y. *Macromolecules* **2003**, 36, 6698.

(18) Song, Y.-H.; Yeh, S.-J.; Chen, C.-T.; Chi, Y.; Liu, C.-S.; Yu, J.-K.; Hu, Y.-H.; Chou, P.-T.; Peng, S.-M.; Lee, G.-H. *Adv. Funct. Mater.* **2004**, in press.

(19) Kan, S.; Liu, X.; Shen, F.; Zhang, J.; Ma, Y.; Zhang, G.; Wang, Y.; Shen, J. *Adv. Funct. Mater.* **2003**, 13, 603.

(20) Gong, X.; Robinson, M. R.; Ostrowski, J. C.; Moses, D.; Bazan, G. C.; Heeger, A. J. *Adv. Mater.* **2002**, 14, 581.



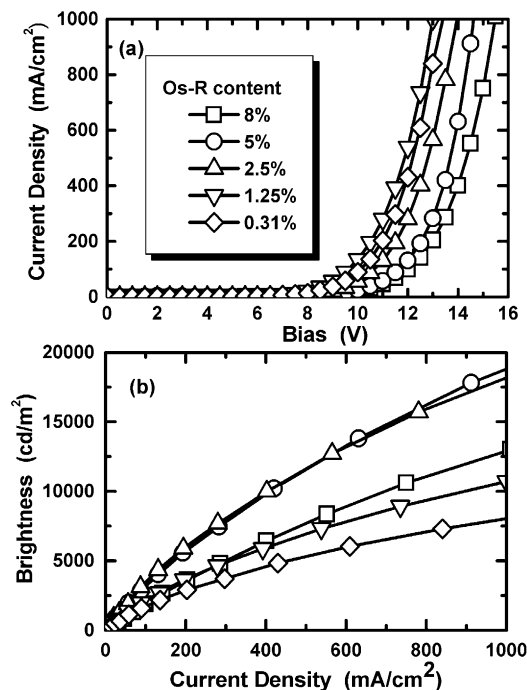


**Figure 3.** (a) Current-density vs voltage (J–V) and (b) brightness vs current-density (B–J) characteristics of the LEDs based on blends with different contents of Os–R in PF–TPA–OXD.

function as a hole-blocking and exciton-confining layer at the cathode side.

The EL spectra corresponding to the LEDs utilizing the blends of Os–R:PF–TPA–OXD as the emitting layer are shown in Figure 2b. In a sharp contrast to the PL spectra, the EL spectra show only the guest  $^3\text{MLCT}$  emission for blends with Os–R content as low as 0.31 wt %. The dramatic difference between the EL and PL spectra is clear evidence of the dominating role of direct charge-trapping and recombination in the EL process over the energy-transfer routes. The main function of the PF–TPA–OXD host is to transport the injected carriers efficiently to the Os–R trap sites dispersed within the entire EL layer, while the transfer of singlet excitons formed on the polymer chains to the  $^3\text{MLCT}$  levels via the  $^1\text{MLCT}$  bridges of the Os complex only plays a minor role. On the other hand, the EL spectrum peaks at 645 nm for the device with 8 wt % Os–R and it blue shifts slightly when the Os–R content is decreased in the blends, to 636 nm for the device with 0.31 wt % Os–R. This is an indication of the decreased interaction among the Os–R molecules. Correspondingly, the CIE coordinates of the emission from the devices operating at 10 mA/cm<sup>2</sup> vary from  $x = 0.670$ ,  $y = 0.328$  (with 8 wt % Os–R) to  $x = 0.668$ ,  $y = 0.332$  (with 2.5 wt % Os–R) and finally to  $x = 0.632$ ,  $y = 0.323$  (with 0.31 wt % Os–R).

The current-density vs voltage (J–V) and brightness vs current-density (B–J) characteristics of the LEDs based on blends with different concentration of Os–R in PF–TPA–OXD are shown in Figures 3a and 3b, respectively. With the increase of Os–R in the blends, the J–V characteristic curves shift gradually to higher voltage, showing that the trapping effect of the Os complex basically decreases the

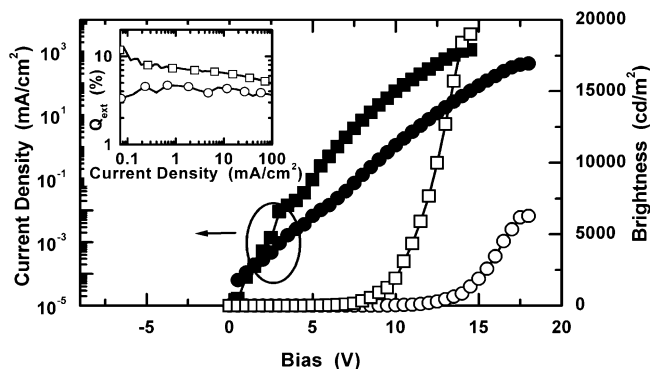


**Figure 4.** Current-density vs voltage (J–V, solid) and brightness vs voltage (B–V, open) characteristics of the LEDs based on blend of 2.5 wt % Os–R in PF–TPA–OXD. The circle corresponds to LED with the structure ITO/PEDOT:PSS/EL layer/TPBI/CsF/Al and the rectangular to ITO/PS–TPD–TFV/EL layer/TPBI/CsF/Al. Inset: External quantum efficiency vs current-density characteristics of the LEDs.

**Table 1.** Performance of LEDs Based on Blend of 2.5 wt % Os Complex in PF–TPA–OXD Device Structure: ITO/HTL(30 nm)/EL Layer(40 nm)/TPBI(25 nm)/CsF(1 nm)/Al(200 nm)

	HTL	PEDOT:PSS	PS–TPD–FTV
turn-on voltage (V)		7.4	4.4
maximum $\eta_{\text{ext}}$ (ph/el %) [LE <sup>a</sup> ]		5.0 [3.4]	12.8 [8.6]
maximum brightness (cd/m <sup>2</sup> )		6,280	19,000
at driving voltage (V)		18.0	14.5
luminance (cd/m <sup>2</sup> )		262	467
at 10 mA/cm <sup>2</sup>			
driving voltage (V)		12.3	8.6
at 10 mA/cm <sup>2</sup>			
$\eta_{\text{ext}}$ (ph/el %) [LE <sup>a</sup> ]			
at 1 mA/cm <sup>2</sup>		4.6 [2.8]	7.5 [5.0]
at 10 mA/cm <sup>2</sup>		4.3 [2.6]	6.9 [4.7]
at 100 mA/cm <sup>2</sup>		3.6 [2.2]	5.3 [3.5]
power efficiency (lm/W)		0.99	2.7
at 1 mA/cm <sup>2</sup>			

<sup>a</sup> Luminous efficiency in cd/A.

carrier transport mobility. The B–J characteristics of the blends with Os–R content below 2.5 wt % show that the device efficiency increases with the increase of Os–R. However, any increase of Os–R beyond 5 wt % has a minor influence on the B–J characteristic, implying that high efficiency can be achieved for blends with Os–R content between ca. 2.5 and 5 wt %. Increasing the Os–R content further to 8 wt % decreases the device efficiency. This indicates that the interaction or aggregation between the Os complex molecules becomes significant at higher concentrations, resulting in the quenching of the triplet emission.<sup>22</sup>

As shown in Figure 4 and Table 1, maximum external quantum efficiency (12.8 ph/el %) at low current density and a maximum brightness above 19000 cd/m<sup>2</sup> were reached with CIE coordinates at  $x = 0.67$ ,  $y = 0.33$ , which are exactly the same as the National Television Systems Committee (NTSC) red standards. Benefiting from the short triplet lifetime and effective dilution of the Os complex (2.5 wt %) in the polymer host, the external quantum efficiency can still retain at 5.3 ph/el % with a brightness of 3498 cd/m<sup>2</sup> even at a high current density of 100 mA/cm<sup>2</sup>.

It is interesting to notice that the control device with PEDOT:PSS as the HTL yielded much lower performance,

(21) Li, Y.; Fung, M. K.; Xie, Z.; Lee, S.-T.; Hung, L.-S.; Shi, J. *Adv. Mater.* **2002**, *14*, 1317.

(22) (a) Connick, W. B.; Geiger, D.; Eisenberg, R. *Inorg. Chem.* **1999**, *38*, 3264. (b) Kalinowski, J.; Stampor, W.; Mezyk, J.; Cocchi, M.; Virgili, D.; Fattori, V.; Di Marco, P. *Phys. Rev. B* **2002**, *66*, 235321.

as shown in Figure 4 and Table 1. Similar contrast was also observed earlier for LEDs based on the iridium complex.<sup>23</sup> Possible reasons for poorer performance may be due to the lack of electron-blocking/exciton confinement at the anode side when PEDOT:PSS is used or unfavorable phase separation between the organometallic complexes and PF-TPA-OXD host that was caused by the hydrophilic nature of the underlying PEDOT:PSS layer. A detailed investigation of the underlying mechanisms for the low performance is underway and the results will be reported elsewhere.

### Conclusion

In conclusion, highly efficient electrophosphorescent LEDs are achieved by blending a neutral Os complex into a single-

component polymer host that possesses balanced hole- and electron-transporting ability. This is the first report on polymer LEDs with saturated red emission and external quantum efficiency greater than 10% based on an organometallic complex other than the iridium core metal. A device structure with both effective hole/electron injection and efficient carriers/excitons blocking or confinement at both electrode sides also contributes significantly to the high performance.

**Acknowledgment.** This work was supported by the National Science Foundation (NSF-STC Program under Agreement Number DMR-0120967) and the Air Force Office of Scientific Research (AFOSR) under the MURI Center on Polymeric Smart Skins. Y. Chi thanks the National Science Council of Taiwan, R.O.C., for the financial support (NSC 91-2119-M-002-016) and (NSC 91-2113-M-007-006). A. K.-Y. Jen thanks the Boeing-Johnson Foundation for its support.

---

(23) Niu, Y.-H.; Chen, B.; Liu, S.; Yip, H.; Bardecker, J.; Jen, A. K.-Y.; Kavitha, J.; Chi, Y.; Song, Y.-H.; Wang, S.-L.; Shu, C.-F.; Tseng, Y.-H.; Chien, C.-H. *Appl. Phys. Lett.* **2004**, *85*, 1619.

CM047709F